AAS 15-364

OPTIMAL LOW-THRUST-BASED RENDEZVOUS MANEUVERS

Juan L. Gonzalo[*], and Claudio Bombardelli[†]

The minimum-time, low-constant-thrust, same circular orbit rendezvous problem is studied using a relative motion description of the system dynamics. The resulting Optimal Control Problem in the thrust orientation angle is formulated using both the Direct and Indirect methods. An extensive set of test cases is numerically solved with the former, while perturbation techniques applied to the later allow to obtain several approximate solutions and provide a greater insight on the underlying physics. These results show that the structure of the solutions undergoes fundamental changes depending on the value of the non-dimensional thrust parameter.

INTRODUCTION

An orbital rephasing maneuver is the modification of the angular position, typically measured in terms of true or eccentric anomaly, of a spacecraft along its orbit while leaving all other orbital elements unchanged at the end of the maneuver. When such modification is small the maneuver is practically equivalent to an equal-orbit rendezvous maneuver in which a spacecraft is moved along its own orbit to reduce the separation distance from a target. This kind of problem is very relevant for different space technology applications and, as a particular case, for the design of future missions performing active debris removal (ADR). Irrespectively of the particular technology employed (e.g. ion beams,[1,2] robotic docking[3]) an ADR mission will always involve a rendezvous phase with a non-cooperative target debris to be removed. Moreover, such operation will most probably need to be conducted in a fully autonomous way. The same-orbit rendezvous problem has been studied extensively in the literature under different perspectives. Most of the literature on the subject deals with impulsive control solutions that have been and are still widely used in practical applications (e.g. V-bar hopping). Nevertheless, recent advances in electric propulsion have raised the interest for minimum-time optimal control solutions entirely based on low-thrust continuous control (for instance, see the works by Lawden[4] or Marec[5]). The use of low-thrust methods, when compatible with the specific spacecraft design considered, can be advantageous not only thanks to the lower propellant consumption but also because it can provide higher maneuvering flexibility in some circumstances. From the mathematical point of view the minimum-time low-thrust control problem is an optimal control problem (OCP) that is typically solved numerically using direct or indirect methods and leading, in general, to a solution with a complex and highly non-intuitive structure. Nevertheless, it has been recently pointed out that the solution can exhibit some interesting characteristics, including an approximate invariance relating the dimensionless thrust and dimensionless time-of-flight for relatively "fast" maneuvers.[6] Clearly, a mathematical investigation of these kinds

[*]PhD candidate, Space Dynamics Group, School of Aerospace Engineering, Technical University of Madrid (UPM).
[†]Research associate, Space Dynamics Group, School of Aerospace Engineering. Technical University of Madrid (UPM).

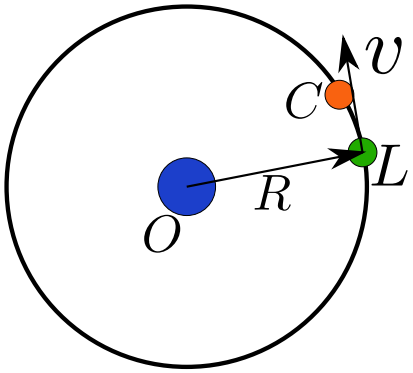

Figure 1. Schematic representation of the problem.

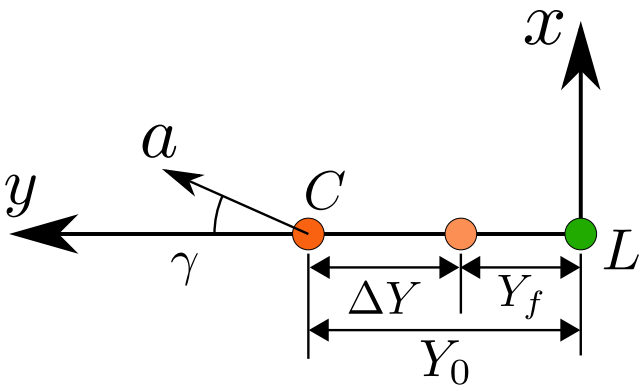

Figure 2. Schematic of the problem in the relative motion reference frame.

of properties using, as much as possible, analytical models would be extremely relevant for future applications of low-thrust rendezvous techniques. One of the key points to facilitate such kind of analysis is the employment of a convenient formulation of the system dynamics linked to the use of perturbation theory as we propose to do in this article. Similarly to other authors,[7,8] the constant-thrust minimum-time rendezvous problem is here formulated starting from the linearized Clohessy-Wiltshire equations written in an orbit reference system coincident with the initial orbit of the leader. A set of numerical solutions to the problem is obtained using a direct collocation method to transcribe the corresponding OCP into a non-linear programing one, which is then solved using a suitable large-scale algorithm. A wide range of non-dimensional thrust parameters is considered, for multiple values of the required angular displacement. Next, an indirect formulation of the OCP is also considered, and several approximate solutions are searched for using perturbation techniques based on the smallness of the dimensionless thrust parameter. These solutions help provide greater insight about the underlying physics of the problem, and confirm the qualitative behaviors detected through the numerical analysis. To conclude the article a qualitative comparison between the low-thrust optimized solution and a two-impulse V-bar rendezvous is presented.

DESCRIPTION OF THE PROBLEM

Consider two objects, a leader L and a chaser C, describing a circular orbit of radius R around a primary with gravitational constant μ. The objective is to perform a rendezvous maneuver, mod-

ifying the position of the chaser to reduce its distance with respect to the chaser. From now on, it will be assumed that the propellant mass expelled from the chaser m_{prop} is negligible compared to its total mass m_C, so the later can be assumed to be constant. Dynamics will be studied using the relative formulation for the motion of the chaser with respect of the leader; to this end, a reference system $\mathcal{R}\{L; \mathbf{i}_R, \mathbf{j}_R, \mathbf{k}_R\}$ is defined, with its origin fixed to the leader, the x axis oriented along its position vector, the y axis coinciding with the velocity vector and the z axis forming a right-handed reference system. A schematic representation of the problem can be seen in Figure 1, while the aforementioned reference frame is depicted in Figure 2. The equations for the planar relative motion of the chaser with respect to the target, projected in reference frame $\mathcal{R}$, take the form:[9]

$$\ddot{x} - 2\Omega\dot{y} - \Omega^2 x = -\frac{\mu\,(R+x)}{\left[(R+x)^2 + y^2\right]^{3/2}} + \frac{\mu}{R^2} + a_x$$
$$\ddot{y} + 2\Omega\dot{x} - \Omega^2 y = -\frac{\mu y}{\left[(R+x)^2 + y^2\right]^{3/2}} + a_y$$

with

$$a = \sqrt{a_x^2 + a_y^2}, \qquad \Omega = \frac{2\pi}{T_{\text{orb}}}, \qquad T_{\text{orb}} = 2\pi\sqrt{R^3/\mu} \tag{1}$$

where a_x and a_y are the perturbing accelerations in the radial and along-track directions respectively, and T_{orb} is the orbital period of the leader.

These equations can be linearized for relatively small values of x and y, leading to the well known equations by Clohessy and Wiltshire:[9]

$$\ddot{x} - 2\Omega\dot{y} - 3\Omega^2 x = a_x$$
$$\ddot{y} + 2\Omega\dot{x} = a_y$$

Is is convenient to express them in a non-dimensional form, introducing:

$$\tau = \Omega t, \quad X = \frac{x}{R}, \quad Y = \frac{y}{R}, \quad A_x = \frac{a_x}{\Omega^2 R}, \quad A_y = \frac{a_y}{\Omega^2 R}, \quad \varepsilon = \frac{a}{\Omega^2 R} \tag{2}$$

which yields:

$$X'' - 2Y' - 3X = A_x$$
$$Y'' + 2X' = A_y$$

Since the objective of the rendezvous maneuver is to reduce the distance between the chaser and the leader while remaining in the same circular orbit, the boundary conditions for a general scenario can be set to be

$$X(0) = 0, \quad Y(0) = Y_0, \quad X'(0) = 0, \quad Y'(0) = 0$$
$$X(\tau_f) = 0, \quad Y(\tau_f) = Y_f = Y_0 + \Delta Y, \quad X'(\tau_f) = 0, \quad Y'(\tau_f) = 0$$

where a negative value of ΔY represents an approach of the chaser with respect to the leader.

Reducing the equations to a first order system, and expressing it in matrix form:

$$\frac{\mathrm{d}}{\mathrm{d}\tau}\begin{bmatrix} U \\ V \\ X \\ Y \end{bmatrix} = \begin{bmatrix} 0 & 2 & 3 & 0 \\ -2 & 0 & 0 & 0 \\ 1 & 0 & 0 & 0 \\ 0 & 1 & 0 & 0 \end{bmatrix}\begin{bmatrix} U \\ V \\ X \\ Y \end{bmatrix} + \begin{bmatrix} A_x \\ A_y \\ 0 \\ 0 \end{bmatrix} \tag{3}$$

$$\frac{\mathrm{d}\mathbf{Z}}{\mathrm{d}\tau} = \mathbf{C}\,\mathbf{Z} + \mathbf{A} = \mathbf{F}$$

where $U = X'$, $V = Y'$ and $\mathbf{Z}$ is the relative state vector of the chaser.

For the purposes of this study, the only perturbing acceleration is the one introduced by the propulsion system of the chaser. Then, it is convenient to express this perturbing acceleration in the form:

$$A_x = \varepsilon \sin\gamma, \quad A_y = \varepsilon \cos\gamma \tag{4}$$

where ε is the non-dimensional magnitude of the thrust acceleration, and γ is its orientation with respect to the along-track direction.

It is interesting to note that Equations (3) can be analytically solved for the unperturbed problem, that is when $\mathbf{A} = \mathbf{0}$. The position and velocity of the chaser with respect to the leader then take the form:

$$\begin{aligned} U &= -\frac{C_3}{2}\cos\tau + \frac{C_4}{2}\sin\tau \\ V &= C_2 + C_3\sin\tau + C_4\cos\tau \\ X &= -\frac{2}{3}C_2 - \frac{C_3}{2}\sin\tau - \frac{C_4}{2}\cos\tau \\ Y &= C_1 + C_2\tau - C_3\cos\tau + C_4\sin\tau \end{aligned} \tag{5}$$

TWO-IMPULSE MANEUVER

For comparison purposes only, two-impulse maneuvers are briefly considered. The boundary conditions for a two-impulse maneuver in the general case take the form:

$$\begin{gathered} X(\tau_0) = 0, \quad Y(\tau_0) = Y_0, \quad U(\tau_0) = \Delta U_0, \quad V(\tau_0) = \Delta V_0 \\ X(\tau_f) = 0, \quad Y(\tau_f) = \Delta Y_f, \quad U(\tau_f) = \Delta U_f, \quad V(\tau_f) = \Delta V_f \end{gathered}$$

where the total distance to be covered in the along-track direction is $\Delta Y = Y_f - Y_0$, negative if the chaser is approaching to the target and positive otherwise. The initial impulse can be better expressed in terms of its magnitude and its orientation angle as:

$$\Delta U_0 = \Delta V \cos\gamma_0\,, \quad \Delta V_0 = \Delta V \sin\gamma_0.$$

Imposing the initial conditions to the general solution given by Equations (5) yields:

$$\begin{aligned} U &= \Delta U_0\cos\tau + 2\Delta V_0\sin\tau \\ V &= -2\Delta U_0\sin\tau + \Delta V_0\,(4\cos\tau - 3) \\ X &= \Delta U_0\sin\tau - 2\Delta V_0\,(\cos\tau - 1) \\ Y &= Y_0 + 2\Delta U_0\,(\cos\tau - 1) + \Delta V_0\,(4\sin\tau - 3\tau) \end{aligned}$$

If the maneuver is to be performed with only two impulses, the fulfillment of the final conditions yields a closed expression for the required initial impulse as a function of the along-track displacement ΔY and the time of flight τ_f:

$$\begin{aligned} \Delta U_0 &= \frac{2\Delta Y\,(\cos\tau_f - 1)}{8\,(1-\cos\tau_f) - 3\tau_f\sin\tau_f} \\ \Delta V_0 &= \frac{2\Delta Y\sin\tau_f}{8\,(1-\cos\tau_f) - 3\tau_f\sin\tau_f} \end{aligned}$$

According to these formulas, for each pair of values $(\Delta Y, \tau_f)$ there is a single initial impulse $(\Delta U_0, \Delta V_0)$ that allows performing the two-impulse transfer maneuver successfully, though the opposite is not true. Moreover, the solution may become singular at those values of τ_f for which the denominator becomes zero. There are two of such roots per revolution: the first one is $\tau_f = 2n\pi$ with $n \in \mathbb{N}$, corresponding to the along-track impulse case presented below, while the other leads to an infinite discrete set of unfeasible solutions in τ_f.

From now, only two strategies will be considered in further detail: using radial impulses or along-track impulses. In the first case, making $\Delta U_0 = \Delta V$ and $\Delta V_0 = 0$:

$$\begin{aligned} U &= \Delta V \cos\tau \\ V &= -2\Delta V \sin\tau \\ X &= \Delta V \sin\tau \\ Y &= Y_0 + 2\Delta V\,(\cos\tau - 1) \end{aligned}$$

The conditions in the final position give the time of flight:

$$\left.\begin{array}{l} X(\tau_f) = 0 \\ Y(\tau_f) \neq Y_0 \end{array}\right\} \quad \Rightarrow \quad \tau_f = \pi + 2n\pi \quad n \in \mathbb{N}$$

that is, the maneuver will take place in half an orbit, plus an arbitrary number of revolutions. The state at this final time is:

$$U(\tau_f) = -\Delta V\,, \quad V(\tau_f) = 0\,, \quad X(\tau_f) = 0\,, \quad Y_f - Y_0 = \Delta Y = -4\Delta V$$

Consequently, the required impulse is given by the along-track displacement to be covered, and a final impulse of magnitude $|\Delta V|$ and the same direction as the first impulse is needed to circularize the orbit:

$$\Delta V = -\frac{\Delta Y}{4}\,, \quad \Delta V_{\text{total}} = 2|\Delta V|\,, \quad X_{\max} = \Delta V\,. \tag{6}$$

Performing the impulse in the along-track direction, $\Delta U_0 = 0$ and $\Delta V_0 = \Delta V$, introduces a secular behavior in Y:

$$\begin{aligned} U &= 2\Delta V \sin\tau \\ V &= \Delta V\,(4\cos\tau - 3) \\ X &= -2\Delta V\,(\cos\tau - 1) \\ Y &= Y_0 + \Delta V\,(4\sin\tau - 3\tau) \end{aligned}$$

The time of flight is again determined by the final condition in the radial position, which being periodic leads to an infinite set of possible solutions:

$$X(\tau_f) = 0 \quad \Rightarrow \quad \tau_f = 2n\pi \quad n \in \mathbb{N} \tag{7}$$

so the maneuver now takes a multiple of an orbit to complete. The rest of the final state variables are:

$$U(\tau_f) = 0\,, \quad V(\tau_f) = \Delta V\,, \quad X(\tau_f) = 0\,, \quad Y_f - Y_0 = \Delta Y = -3\Delta V \tau_f$$

so the required impulse and the maximum radial displacement take the form:

$$\Delta V = -\frac{\Delta Y}{3\tau_f}\,, \quad \Delta V_{\text{total}} = 2|\Delta V|\,, \quad X_{\max} = 4\Delta V\,. \tag{8}$$

This solution shows some key differences with the radial one. First of all, the distance covered now depends on time, which allows to reduce fuel consumption by performing the rendezvous in multiple revolutions. Furthermore, Figure 5 shows that along-track impulses correspond to the local minimum of ΔV for a given number of revolutions. On the other hand, this introduces some operational risks, since the spacecraft could be lost if the second impulse is not or cannot be performed at the proper time. Also noteworthy is that the final instant does not coincide with the maximum approach between leader and target, introducing further operational risks. Finally, regarding the direction of the impulses, the second one must be performed in the direction opposite to the first one, requiring the spacecraft to change attitude or to have an opposing set of thrusters.

CONTINUOUS THRUST MANEUVER

For the rest of this paper, the Optimal Control Problem (OCP) of performing a minimum-time rendezvous maneuver using continuous, constant thrust acceleration is studied. Since the mass of the chaser is assumed to be constant, this is also equivalent to minimizing the total impulse required for the maneuver. A wide range of perturbing accelerations is considered, not limiting it to the low thrust case. While this includes some results of little practical interest, it allows to reach a deeper understanding of the problem and its characteristics.

First of all, the problem is solved numerically using the Direct Method. Then, the equations for the Two-Point Boundary Value Problem derived from the Indirect Method are posed, and a set of approximate solutions are reached. Both paths yield interesting information about the problem and the qualitative changes it undergoes as the thrust acceleration varies.

Direct Method

Numerical solutions for the OCP can be obtained by performing a direct transcription[10] and solving the resulting discrete Non-Linear Programming (NLP) problem with a suitable algorithm. To this end, the continuous functions for the state and control are represented through their values at the points (and middle-points, depending on the scheme used) of a uniformly spaced grid between 0 and τ_f. The optimization variable $\boldsymbol{\chi}$ is then formed by the values of the state and control at each grid point (and middle-points for certain schemes), as well as the final time:

$$\boldsymbol{\chi} = \begin{pmatrix} \tau_f & \mathbf{Z}^1 & \gamma^1 & \dots & \mathbf{Z}^k & \gamma^k & \dots & \mathbf{Z}^M & \gamma^M \end{pmatrix}$$

where

$$\mathbf{Z}^k = \mathbf{Z}(\tau^k)\,, \quad \gamma^k = \gamma(\tau^k)\,, \quad \tau_k = \frac{k-1}{M-1}\tau_f$$

with M being the number of nodes. The equations of dynamics are also discretized using implicit Runge-Kutta schemes, and imposed as a set of non-linear equality constraints called *defect constraints*:

$$\boldsymbol{\xi}(\boldsymbol{\chi}) = \mathbf{0}.$$

From now on, the Trapezoidal and Hermite-Simpson Separated schemes will be used; for a brief description of said algorithms, see the Appendix. No other path constraints are needed for this problem, only bound constraints for the values of the state at the extremal nodes of the grid. The objective or cost function for a minimum time maneuver is also straightforward to define, being equal to the first element of the optimization variable:

$$J = \chi_1 = \tau_f.$$

The NLP algorithm requires the Jacobian and Hessian of the objective function and the constraints (or a suitable approximation). Since the only constraints are those coming form the discretization of dynamics, and the corresponding equations are relatively simple, the Jacobian is built analytically, giving raise to a sparse matrix whose size and structure depends on the transcription algorithm. On the other hand, the Hessian will be approximated numerically from the Jacobian using the procedure proposed by Coleman, Garbow and Moré,[11] which also leverages sparsity to minimize the number of evaluations.

The resulting NLP problem is numerically solved using a third party software package, particularly MATLAB's global optimization toolbox and its *interior point* algorithm. The algorithm selection is based on its support for sparse, large scale problems, which is of great importance for problems coming from the discretization of dynamical systems.

A set of problems is now solved for a circular reference orbit around the Earth with:

$$R = 7000\,\text{km}\,, \quad T_{\text{orb}} = 97.142\,\text{min}\,, \quad \Omega = 1.078\,10^{-3}\,\text{rad/s}$$

and an initial separation between the chaser and the leader of

$$\Delta y = -700\,\text{m}\,, \quad \Delta Y = \frac{\Delta y}{R} = -10^{-4}$$

where the minus sign indicates that the chaser is in front of the leader. For simplicity sake, it is assumed that the final along-track distance between leader and chaser must be zero. Note that, given the characteristic value taken for distance, the non-dimensional separation coincides with the angular phase between chaser and leader measured in radians. A wide range of non-dimensional thrust acceleration parameters $\varepsilon \in [10^{-1}, 10^{-9}]$ is considered, corresponding to physical accelerations between $8.1347\,10^{-1}$ m/s^2 and $8.1347\,10^{-9}$ m/s^2. To improve the numerical convergence of the NLP solver a continuation of solutions scheme is followed, using each solution as initial guess for the next case. A 500-nodes grid and the Hermite-Simpson Separated method are used, while the Trapezoidal method is employed to construct the first initial guess for $\varepsilon = 10^{-1}$. The use of the HSS method not only provides a higher order discretization of dynamics, but also allows to estimate the costate (see the following section on the Indirect formulation of the problem) from the Lagrange multipliers in the NLP algorithm.

The evolution with ε of the time needed to perform the maneuver τ_f is represented in Figure 3. It is straightforward to distinguish two different regimes, which may be called high thrust and low thrust regimes. As it is studied in the following section using the Indirect formulation, the former is dominated by thrust, while gravitational effects play a key role in the latter. This study also yields approximate predictions for τ_f in each regime, which are represented as discontinuous lines. The transition zone between the two regimes take place for values of τ_f around one orbit, which corresponds to $\tau_f = 2\pi$. Regarding the total impulse needed to perform the maneuver, Figure 4 shows that it decreases as the time of flight increases, with the gravity dominated regime being more efficient that the thrust dominated one. Consequently, using a low-thrust propulsion system allows a significant reduction of ΔV, and an even greater improvement in propellant mass if the higher specific impulse of said engines is taken into account, at the cost of a longer mission time.

It is also interesting to compare the ΔV required to perform a given maneuver using either impulsive or continuous thrust. Figure 5 shows the evolution with the time of flight of the ΔV needed in each case to achieve a total along-track displacement of $\Delta Y = -10^{-4}$. It is checked that the curve for the two-impulse maneuver varies greatly with τ_f, having one vertical asymptote and one

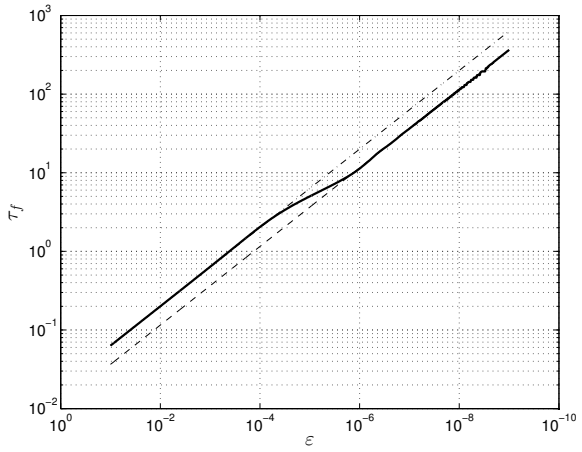

Figure 3. Time of flight τ_f as a function of the thrust parameter ε, for a total displacement of $\Delta Y = -10^{-4}$

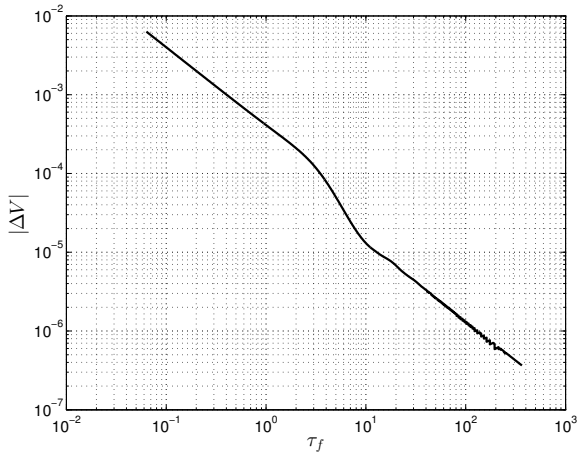

Figure 4. Required total impulse ΔV as a function of the time of flight τ_f, for a total displacement of $\Delta Y = -10^{-4}$

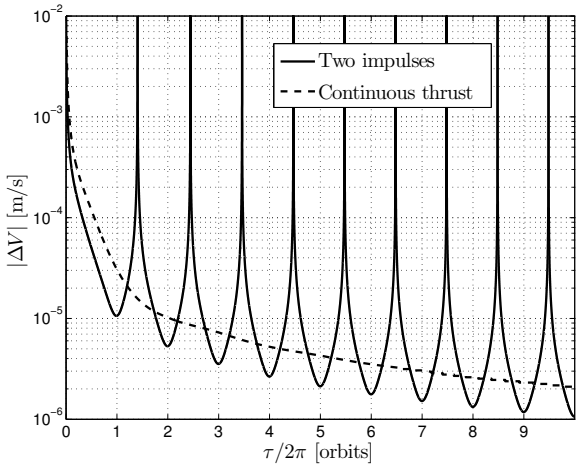

Figure 5. Comparison of the total ΔV required for a displacement of $\Delta Y = -10^{-4}$ using impulsive and continuous thrust.

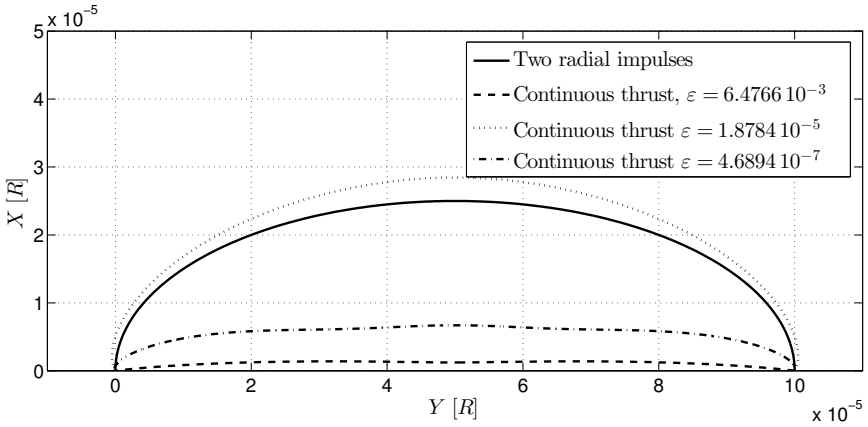

Figure 6. In-plane trajectories with $\Delta Y = -10^{-4}$, for a two-radial-impulses maneuver and three different continuous thrust maneuvers.

minimum per revolution, while the continuous thrust maneuver evolves in a much smoother way. Owing to the great ΔV variability of the impulsive maneuver, it may perform better or worse than the continuous thrust case depending on the particular value of τ_f, though it is clear that the minimum values at each revolution are reached using along-track impulses. Both this minima and the curve for the continuous maneuver evolve with τ_f in a similar fashion, presenting their steepest variations for short mission times.

The in-plane trajectories corresponding to the two-radial-impulses maneuver and three different continuous thrust maneuvers are represented in Figure 6. The maximum radial displacement of the continuous thrust maneuvers remains small compared to the impulsive case for values of ε in the thrust-dominated and gravity-dominated regimes ($6.4766\,10^{-3}$ and $4.689\,10^{-7}$ respectively), while it becomes comparable and even slightly larger in the transition zone ($6.4766\,10^{-3}$). It is also noteworthy that the trajectories for $\varepsilon = 6.4766\,10^{-3}$ and $\varepsilon = 4.689\,10^{-7}$ have a minimum along-track distance with respect of the target slightly smaller than the final separation, and that they start moving in the opposite direction at the beginning of the maneuver.

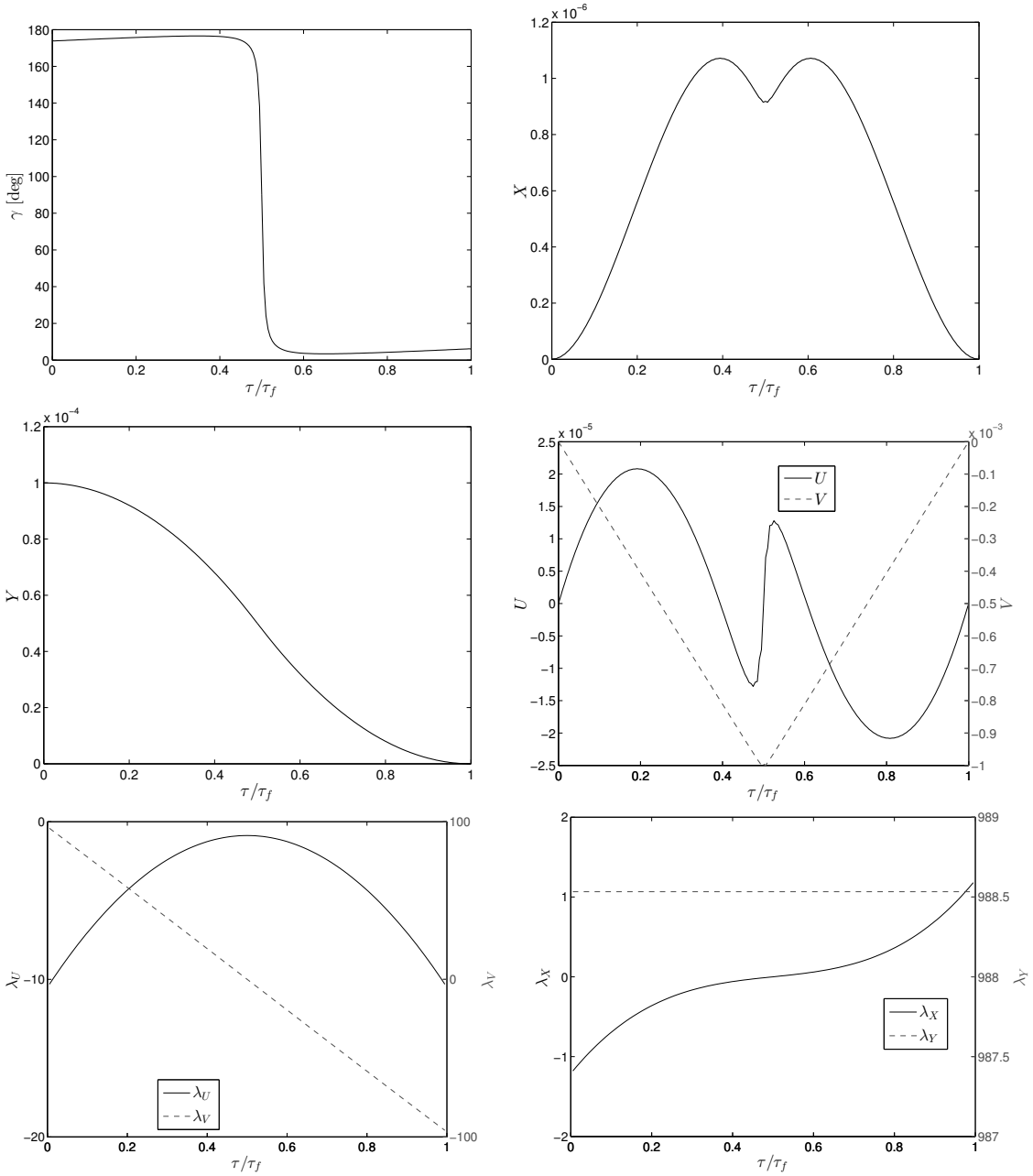

Figure 7. Solutions obtained for $\Delta Y = -10^4$ and $\varepsilon = 1.0273\,10^{-2}$.

To conclude this part of the study, three particular cases taken from each of the regimes and the transition zone are considered. Figures 7 show the thrust angle, state (position and velocities) and costate for a thrust parameter of $\varepsilon = 1.0273\,10^{-2}$, corresponding to a physical acceleration of $a = 8.3566\,10^{-2}\,\mathrm{m/s^2}$ and a maneuver time of $\tau_f = 0.1974$. It is observed that the control approaches a step function, with the switch taking place at the middle of the maneuver. During the first half of the maneuver, thrust is orientated towards the leader, while in the second half its direction is reversed to circularize the orbit. The profiles for X, U and V show clear symmetries, while the short time span of the rendezvous prevents the gravity-dominated effects to fully develop.

The form of the solution undergoes fundamental changes in the gravity-dominated case. Figures 9, calculated for $\varepsilon = 1.0077\,10^{-7}$, which means $a = 8.1975\,10^{-7}\,\mathrm{m/s^2}$ and $\tau_f = 36.2702$, show that the thrust angle profile, while still being close to a step function, has reversed its direction. It points opposite to the leader during the first half of the maneuver, and towards it in the second. The reason is that, since gravitational effects are of great importance in this regime, the minimum-time maneuver is achieved using thrust to produce a radial displacement which in turn introduces a relative velocity towards the leader. The profiles for the state are still symmetric, but now the oscillations due to the gravitational effects in the relative motion can be clearly appreciated.

Finally, Figures 8 correspond to a rendezvous in the transition zone, with $\varepsilon = 1.0194\,10^{-4}$, $a = 8.2926\,10^{-4}\,\mathrm{m/s^2}$ and $\tau_f = 2.0253$. The thrust angle profile no longer resembles a step function, showing important components in the radial direction. Nevertheless, the symmetry between the first and second halves of the maneuver is conserved, and the curves for X and Y are similar to those obtained for the previous examples.

Indirect Method

The OCP is now studied using the Indirect formulation. According to the classic text by Bryson and Ho,[12] a cost function corresponding to minimum maneuver time can be defined in the form:

$$J = \phi + \int_0^{\tau_f} L\,\mathrm{d}\tau = \tau_f\,, \quad L = 1,\ \phi = 0$$

where ϕ would represent the dependence of the cost function with the final state (in this case there is no such dependence). The associated Hamiltonian can then be written as:

$$H = \boldsymbol{\lambda}^\top \mathbf{F} + L = \lambda_U\,(2V + 3X + A_x) + \lambda_V\,(-2U + A_y) + \lambda_X U + \lambda_Y V + 1 \tag{9}$$

where $\boldsymbol{\lambda} = (\lambda_U, \lambda_V, \lambda_X, \lambda_Y)$ is the costate associated to the state $\mathbf{Z}$.

For the solution to be optimum, it must fulfill the first order optimality conditions given by the Euler-Lagrange equations. From the definition given for the Hamiltonian, the adjoint equations are

$$\dot{\boldsymbol{\lambda}} = -\frac{\partial H}{\partial \mathbf{Z}} \Rightarrow \begin{array}{l} \dot{\lambda}_U = 2\lambda_V - \lambda_X \\ \dot{\lambda}_V = -2\lambda_U - \lambda_Y \\ \dot{\lambda}_X = -3\lambda_U \\ \dot{\lambda}_Y = 0 \end{array} \tag{10}$$

the control equation

$$0 = \frac{\partial H}{\partial \gamma} \Rightarrow 0 = \varepsilon\lambda_U \cos\gamma - \varepsilon\lambda_V \sin\gamma \Rightarrow \tan\gamma = \frac{\lambda_U}{\lambda_V} \tag{11}$$

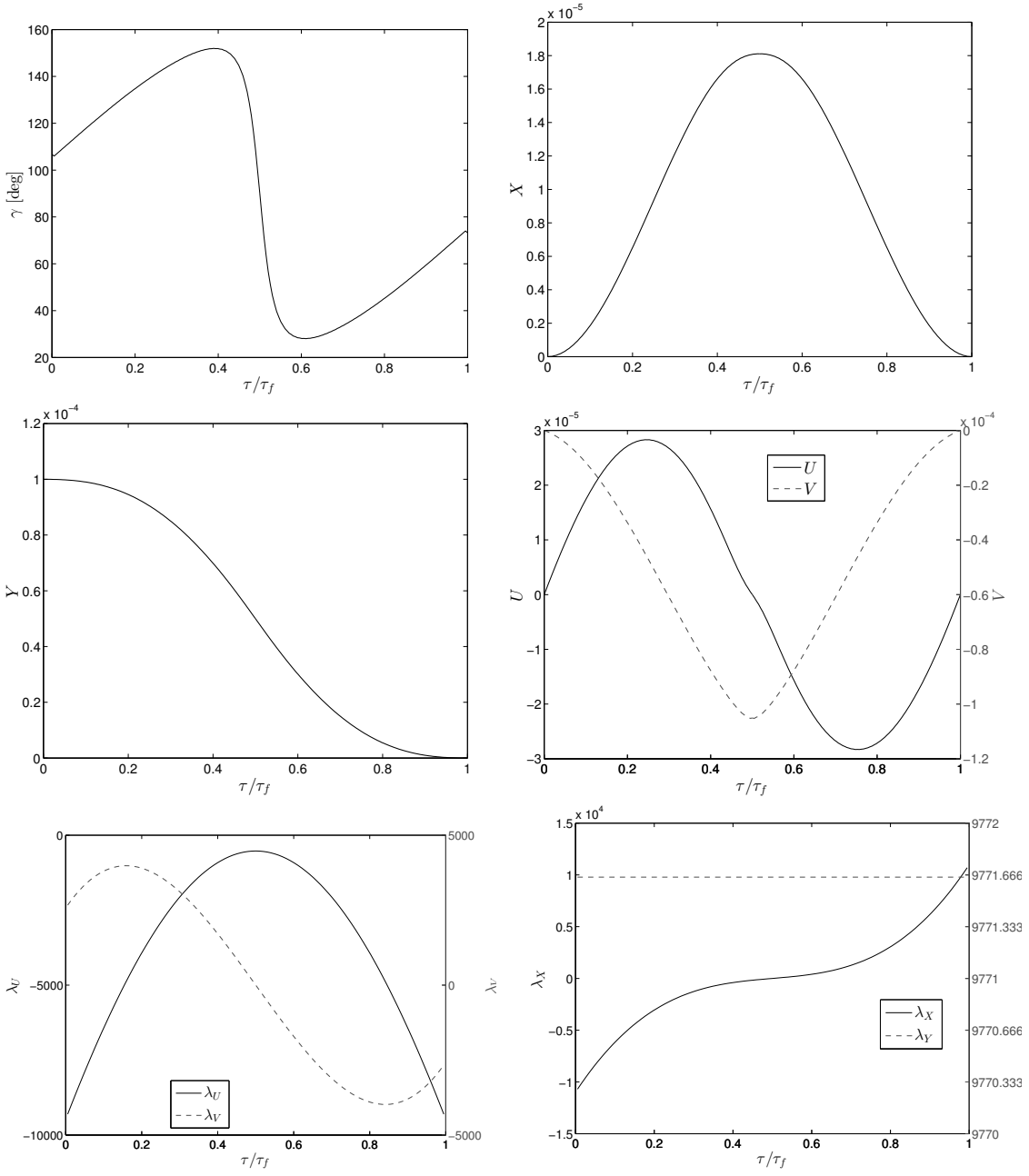

Figure 8. Solutions obtained for $\Delta Y = -10^4$ and $\varepsilon = 1.0194\,10^{-4}$.

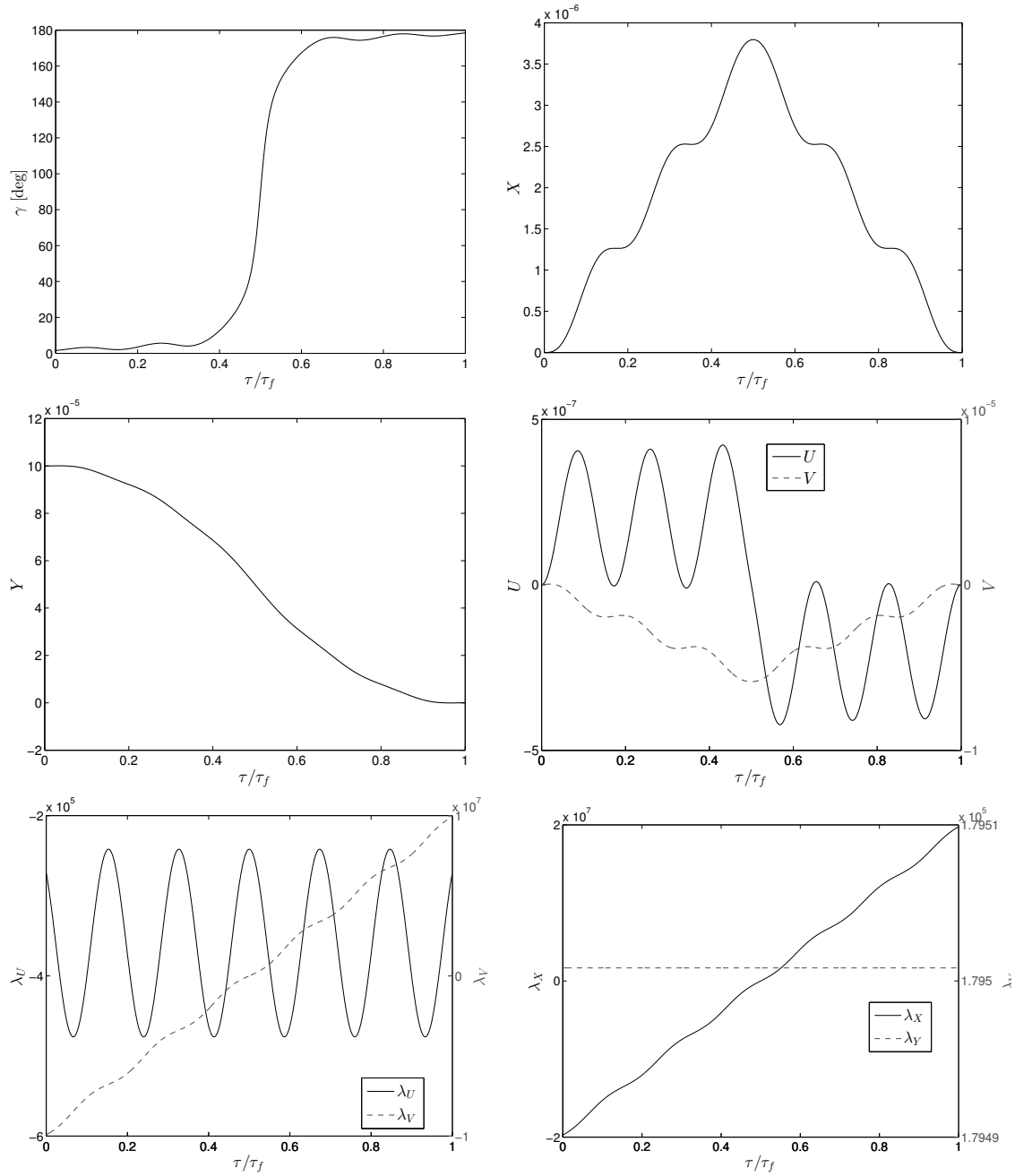

Figure 9. Solutions obtained for $\Delta Y = -10^4$ and $\varepsilon = 1.0077\,10^{-7}$.

and the transversality condition introduced by the minimum-time requirement

$$\left(\frac{\partial \phi}{\partial \tau} + H\right)_{\tau_f} = 0 \Rightarrow \boldsymbol{\lambda}^\top \mathbf{F}\Big|_{\tau_f} = -1\,. \tag{12}$$

Together with the equations for dynamics and the boundary conditions for the state

$$\mathbf{Z}(0) = \begin{pmatrix} 0 & 0 & 0 & Y_0 \end{pmatrix} \quad , \qquad \mathbf{Z}(\tau_f) = \begin{pmatrix} 0 & 0 & 0 & Y_f \end{pmatrix} \tag{13}$$

these equations form a differential-algebraic system of eight ODEs, Equations (3) and (10), and two algebraic Equations (11) and (12). Note that, since the state is fully specified at both the initial and final times, there are no boundary conditions for the costate.

Through careful manipulation of Equation (11), expressions for $\sin\gamma$ and $\cos\gamma$ which take into account the angular determination can be reached:

$$\sin\gamma = -\mathrm{sgn}\,(\varepsilon)\,\frac{\lambda_U}{\sqrt{\lambda_U^2 + \lambda_V^2}}\,, \quad \cos\gamma = -\mathrm{sgn}\,(\varepsilon)\,\frac{\lambda_V}{\sqrt{\lambda_U^2 + \lambda_V^2}} \tag{14}$$

Assuming that the state constraints at the final time are fulfilled, and substituting Equations (4), the transversality condition takes a simpler form:

$$\lambda_U \varepsilon \sin\gamma + \lambda_V \varepsilon \cos\gamma + 1\big|_{\tau_f} = 0\,,$$

and introducing the known expressions for $\sin\gamma$ and $\cos\gamma$:

$$\lambda_U(\tau_f)^2 + \lambda_V(\tau_f)^2 = \frac{1}{\varepsilon^2}\,. \tag{15}$$

The equations for the costate are linear, and can be straightforwardly integrated to yield

$$\begin{aligned}
\lambda_U &= A\sin(\tau + \varphi) - 2B \\
\lambda_V &= 2A\cos(\tau + \varphi) + 3B\tau + C \\
\lambda_X &= 3A\cos(\tau + \varphi) + 6B\tau + 2C \\
\lambda_Y &= B
\end{aligned}$$

Since the initial and final costates are unknowns of the problem, the solution depends on four parameters which would be determined by imposing the boundary conditions for the state. It is interesting to highlight that the form of these solutions matches with the numerical examples given in Figures 7-9.

Introducing these developments, the OCP is now expressed as a Two-Point Boundary Value Problem given by the dynamics, differential Equations (3), and the transversality condition, algebraic Equation (15), with five unknowns τ_f, A, B, C and φ. The system is non-linear due to the terms associated with the control, and cannot be solved analytically: a numerical solution could be searched for using methods such as shooting. Nevertheless, since the problem has already been numerically solved using the Direct method, the rest of this section is devoted to extracting more information about the problem by examining these equations without solving them.

It is very convenient to obtain a first estimation on the value of τ_f to serve as an initial guess for the iterative procedures involved in both the Direct and Indirect method. Such an estimate, as well as

more insight on the physics of the problem, can be obtained from the equations for dynamics under certain assumptions. The order of magnitude for each term in the linear, second order equations for dynamics can be expressed as follows:

$$\underbrace{\frac{\mathrm{d}X'}{\mathrm{d}\tau}}_{\frac{\Delta X}{\Delta\tau^2}} = \underbrace{2Y'}_{2\frac{\Delta Y}{\Delta\tau}} + \underbrace{3X}_{3\Delta X} + \underbrace{\varepsilon \sin\gamma}_{\varepsilon u_x} \quad , \qquad \underbrace{\frac{\mathrm{d}Y'}{\mathrm{d}\tau}}_{\frac{\Delta Y}{\Delta\tau^2}} = -\underbrace{2X'}_{2\frac{\Delta X}{\Delta\tau}} + \underbrace{\varepsilon \cos\gamma}_{\varepsilon u_y} \tag{16}$$

where $|u_x|, |u_y| \ll 1$ and, since $\tau_0 = 0$, $\Delta\tau \simeq \tau_f$. Considering the second equation first, the limit cases where movement in the along-track direction is dominated by either gravitational or thrust effects can be distinguished. In the former case

$$\Delta X \sim \Delta Y/\tau_f$$

and the orders of magnitude for the first equation read:

$$1 \quad 2\tau_f^2 \quad 3\tau_f^2 \quad \frac{\varepsilon}{\Delta Y}\tau_f^3 u_x$$

Taking into account that the term coming from control must be at least as important as the rest, we can distinguish three cases. If $\varepsilon \gg \Delta Y$, the terms associated to acceleration and control are dominant yielding $\tau_f \sim \sqrt[3]{\Delta Y/(\varepsilon u_x)}$. If $\varepsilon \sim \Delta Y$ all terms are comparable and $\tau_f \sim 1$. For $\varepsilon \ll \Delta Y$, the term associated to acceleration is negligible compared to the rest, and $\tau_f \sim \Delta/(\varepsilon u_x)$. In all cases, it is seen that the time of flight is minimized by taking $u_x \sim 1$.

The case where movement in the along-track direction is dominated by the control acceleration proves to be more interesting. From the second equation

$$\tau_f \sim \sqrt{\frac{\Delta Y}{\varepsilon u_y}} \tag{17}$$

so minimum time requires $u_y \sim 1$, which also implies $|u_x| \ll 1$. The orders of magnitude for the first equation are now

$$\frac{\Delta X}{\Delta Y} \quad 2\sqrt{\frac{\Delta Y}{\varepsilon}} \quad \frac{\Delta X}{\Delta Y}\frac{\Delta Y}{\varepsilon} \quad u_x$$

Same as before, we can consider three cases depending on the relation between ε and ΔY. When $\varepsilon \gg \Delta Y$, the time of flight required to perform the maneuver is small, $\tau_f \ll 1$, and the terms in the first equation associated to the radial acceleration and the along-track velocity dominate over the others, yielding $\Delta X \sim \Delta Y \tau_f$. Regarding the along-track equation, $\Delta X \tau_f \sim \Delta Y \tau_f^2$, which is in fact negligible versus $\varepsilon\tau_f^2$, justifying the approximation of considering thrust as the dominant term. Conversely, for $\varepsilon \ll \Delta Y$ the time required to perform the maneuver is greater than one orbit, $\tau_f \gg 1$, and the dominant terms in the radial equation are those coming from the radial position and the along-track velocity, so $\Delta X \sim \Delta Y/\tau_f$. In this case the Coriolis term in the along-track equation is not negligible but coupled with thrust, since $\Delta X \tau_f \sim \Delta Y$ is of the same order as $\varepsilon\tau_f^2$. In both cases considered so far, the along-track velocity term in the radial equation is at least as important as the rest, representing the coupling with the control (which is mostly applied in the along-track direction). Finally, when $\varepsilon \sim \Delta Y$ the limit case of $\tau_f \sim 1$ is reached, and all terms are of comparable order in both equations.

From the previous estimates for τ_f, it is concluded that flight time for the cases where $\varepsilon \ll \Delta Y$ or $\varepsilon \gg \Delta Y$ is minimized by orienting thrust around the along-track direction, leading to a regime where thrust acceleration is at least as important as the rest of terms in the along-track equation. On the other hand, in the intermediate case where $\varepsilon \sim \Delta Y$ both strategies yield $\tau_f \sim 1$, showing that there is no preferent orientation for thrust.

A better estimate on τ_f can be obtained by solving the simplified equations which arise from neglecting the non-dominant terms in dynamics. Considering the low-thrust, or gravity-dominated, case first, $\varepsilon \ll \Delta Y$, the acceleration and thrust terms in the radial equation can be neglected, so said equation reduces to

$$Y' = -\frac{3}{2}X$$

This is consistent with the numerical results in Figures 9, and shows that the along-track velocity is obtained through the radial displacement, which in turn is obtained by applying thrust in the direction opposite to that in which we want to move. The later effect can be seen by considering the along-track equation, which after substituting the previous result takes the form:

$$-\frac{3}{2}X' + 2X' = A_y \quad \Rightarrow \quad X' = 2A_y$$

The order of the differential equations has been reduced by neglecting the non-dominant terms, and so the boundary conditions for velocity cannot be imposed. Coincidentally, said conditions are fulfilled in the along-track direction, but will never be in the radial direction. Assuming A_y is constant, the previous equations can be solved to yield

$$X = X_0 + 2A_y\tau$$

$$Y = Y_0 - \frac{3}{2}X_0\tau - \frac{3}{2}A_y\tau^2$$

This approximate solution does not show the oscillatory behavior present in the numerical results, but succeeds in capturing the evolution of the mean value of the state. The boundary condition in X can be fulfilled by taking $A_y = \varepsilon$ during the first half of the motion, and $A_y = -\varepsilon$ during the second half

$$X\left(\tau_f/2\right) = \varepsilon\tau_f \quad , \qquad X\left(\tau_f\right) = -\varepsilon\tau_f + \varepsilon\tau_f = 0$$

which yields for the along-track position

$$Y\left(\tau_f/2\right) = Y_0 - \frac{3}{8}\varepsilon\tau_f^2 \quad , \qquad Y\left(\tau_f\right) = Y_f = -\frac{3}{4}\varepsilon\tau_f^2 + Y_0$$

This gives an estimate for the time of flight of

$$\tau_f = \sqrt{-\frac{4}{3}\frac{\Delta Y}{\varepsilon}} \tag{18}$$

which fits very well with the numerical results. Interestingly, the minus sign inside the square root indicates that the orientation of thrust during the first half of the maneuver must be *opposite* to the desired displacement of the spacecraft. Regarding the cost of the maneuver, the total impulse can be easily computed for the constant thrust case as

$$\Delta V = \varepsilon\tau_f = \sqrt{-\frac{4}{3}\varepsilon\Delta Y} \tag{19}$$

Comparing this results with the two-radial-impulse reference solution previously presented, it is straightforward to conclude that the low-thrust maneuver presents a lower ΔV requirement, at the cost of a higher time of flight. Moreover, the ratio between both cases is $\Delta V_{\text{cont.}}/\Delta V_{\text{imp.}} \propto 1/\tau_{f\text{imp.}}$, showing that the total impulse evolves with the inverse of the time of flight for a fixed displacement. The total impulse for both cases becomes comparable for $\varepsilon \sim \Delta Y$, the limit case between the two regimes observed for the constant thrust maneuver.

In the high-thrust, or thrust-dominated, regime, when $\varepsilon \gg \Delta Y$, the Coriolis term in the along-track equation is negligible. This leads to an equation which can be solved for constant A_y:

$$Y'' = A_y \quad \Rightarrow \quad \begin{cases} Y' = A_y\tau + Y_0' \\ Y = \dfrac{1}{2}A_y\tau^2 + Y_0'\tau + Y_0 \end{cases}$$

Regarding the radial equation, the term associated to the radial displacement is negligible, while the perturbing acceleration can be at most of the same order of the other two for $u_x \sim \tau_f$. Assuming that $u_x \ll \tau_f$:

$$X'' = Y' \quad \Rightarrow \quad \begin{cases} X' = A_y\tau^2 + 2Y_0'\tau + X_0' \\ X = \dfrac{1}{3}A_y\tau^3 + Y_0'\tau^2 + X_0'\tau + X_0 \end{cases}$$

Taking once again $A_y = \varepsilon$ during the first half of the maneuver and $A_y = -\varepsilon$ during the second half yields

$$\begin{gathered} Y'(\tau_f/2) = \frac{\varepsilon}{2}\tau_f\,, \quad Y(\tau_f/2) = Y_0 + \frac{\varepsilon}{8}\tau_f^2 \\ X'(\tau_f/2) = \frac{\varepsilon}{4}\tau_f^2\,, \quad X(\tau_f/2) = \frac{\varepsilon}{24}\tau_f^3 \\ Y'(\tau_f) = 0\,, \quad Y(\tau_f) = Y_f = \frac{\varepsilon}{4}\tau_f^2 + Y_0 \\ X'(\tau_f) = \frac{\varepsilon}{2}\tau_f^2\,, \quad X(\tau_f) = \frac{\varepsilon}{4}\tau_f^3 \end{gathered}$$

Boundary conditions in the radial direction are not fulfilled, appearing errors in both the final velocity and position (with the later being smaller than the former). A control with $u_x \sim \tau_f \ll 1$ would have the required order of magnitude to interact with the rest of terms and, properly chosen, cancel the errors, while still being oriented very close to the along-track direction. From the final value for the along-track position is possible to give an estimate for the time of flight

$$\tau_f = 2\sqrt{\frac{\Delta Y}{\varepsilon}} \tag{20}$$

which represents a very good approximation of the numerical results obtained in Figure 3. It is very interesting to highlight that thrust is now initially oriented in the *same* direction as the desired displacement of the spacecraft, which represents a *qualitative* change with respect to the solution obtained for the gravity-dominated low-thrust regime. The total impulse required for this maneuver is of the form

$$\Delta V = 2\sqrt{\varepsilon \Delta Y} \tag{21}$$

so it is greater than the corresponding total impulse for the reference two-radial-impulses maneuver. Same as for the low-thrust case, this is related with the fact that the ratio between total impulses

evolves as the inverse of the time of flight, $\Delta V_{\text{cont.}}/\Delta V_{\text{imp.}} \propto 1/\tau_{f\text{imp.}}$. Once again, both total impulses become comparable in the limit case $\varepsilon \sim \Delta Y$.

The previous analysis shows the existence of a transition zone between the two regimes for $\varepsilon \sim \Delta Y$, that is, when $\tau_f \sim 1$, but provides little information about the behavior of the solution during said transition. From a qualitative point of view, it is no longer true that $|A_y| \sim \varepsilon$ and $|A_x| \ll 1$, so the control angle γ may take any value instead of remaining close to the along-track direction. Furthermore, fundamental qualitative changes take place when moving from one regime to the other through the transition zone, the most notable being the reversal of the orientation of thrust. In any case, a detailed description of this transition zone would require solving the complete TPVBP associated to the OCP, and goes beyond the scope of this work.

CONCLUSION

The minimum time constant thrust rendezvous problem in circular orbit has been analyzed in great detail with the aid of a relative motion formulation and using both a direct and an indirect approach. Results show that the structure of the solution undergoes a fundamental qualitative change as the thrust parameter varies, being possible to distinguish two different regimes, a thrust-dominated and a gravity-dominated one, with a transition zone between them. Far from this transition zone, the thrust orientation control law follows a nearly bang-bang structure, with the direction of the jumps being reversed between the two limit regimes. A clear relation between the required maneuver time and the thrust parameter is also observed for both regimes. Finally, an analytical approximation of the relation between required maneuver time and thrust parameter is proposed which may be very useful to quickly assess the main characteristics of a low-thrust rendezvous maneuver even before performing any optimization and to perform trade-off analyses with impulsive techniques.

ACKNOWLEDGMENT

This work has been supported by the Spanish Ministry of Education, Culture and Sport through its FPU Program (reference number FPU13/05910), and by the Spanish Ministry of Economy and Competitiveness within the framework of the research project "Dynamical Analysis, Advanced Orbital Propagation, and Simulation of Complex Space Systems" (ESP2013-41634-P). The authors also want to thank the funding received from the European Union Seventh Framework Programme (FP7/2007-2013) under grant agreement N 607457 (LEOSWEEP).

APPENDIX: TRANSCRIPTION ALGORITHMS FOR DYNAMICS

The direct transcription of an OCP implies expressing dynamics as a set of non-linear constraints using a suitable integration scheme, normally from the implicit Runge-Kutta family. Implicit algorithms are preferred over explicit ones because of their greater order for the same number of stages and better stability, both being very desirable properties for a NLP formulation. On the other hand, while they normally require a higher computational cost, this is not relevant in this context due to the iterative nature of the NLP algorithms.

The first algorithm used in this study is the *Trapezoidal Method*, a 2-stages, 3rd order, Implicit Runge-Kutta scheme given by the equation

$$\mathbf{Z}^{k+1} = \mathbf{Z}^{k+1} + \frac{\tau^{k+1} - \tau^k}{2} \left(\mathbf{F}^{k+1} + \mathbf{F}^k \right)$$

where

$$\mathbf{F}^k = \mathbf{F}\left(\mathbf{Z}^k, \gamma^k, \tau^k\right)$$

The resulting defect constraint is then

$$\boldsymbol{\xi}^k(\chi) \equiv \mathbf{Z}^{k+1} - \mathbf{Z}^{k+1} - \frac{\tau^{k+1} - \tau^k}{2}\left(\mathbf{F}^{k+1} + \mathbf{F}^k\right) = 0. \tag{22}$$

There is a set of defect constraints for each grid node except the last one, and since the state vector $\mathbf{Z}$ has dimension 4 the total number of defect constraints is $4(M-1)$, where M is the number of nodes in the grid.

The *Hermite-Simpson Separated Method* employs a 3-stages, 4^{th} order Implicit Runge-Kutta scheme. It shows the peculiarity of introducing the values of the state and control at the middle-points of the grid as part of the optimization variable $\boldsymbol{\chi}$, being this its main difference with the Hermite-Simpson Compressed Method (which only adds the control). The main equations for this method are

$$\mathbf{0} = \overline{\mathbf{Z}}^{k+1} - \frac{1}{2}\left(\mathbf{Z}^{k+1} + \mathbf{Z}^{k+1}\right) - \frac{\tau^{k+1} - \tau^k}{8}\left(\mathbf{F}^{k+1} - \mathbf{F}^k\right) \quad \text{Hermite interpolant}$$

$$\mathbf{0} = \mathbf{Z}^{k+1} - \mathbf{Z}^{k+1} - \frac{\tau^{k+1} - \tau^k}{6}\left(\mathbf{F}^{k+1} + 4\overline{\mathbf{F}}^{k+1} + \mathbf{F}^k\right) \quad \text{Simpson quadrature}$$

where the line denotes values evaluated at the middle-point between τ^k and τ^{k+1}. These equations give raise to eight defect constraints at each node except the last one

$$\boldsymbol{\xi}^k(\boldsymbol{\chi}) = \begin{bmatrix} \overline{\mathbf{Z}}^{k+1} - \frac{1}{2}\left(\mathbf{Z}^{k+1} + \mathbf{Z}^{k+1}\right) - \frac{\tau^{k+1}-\tau^k}{8}\left(\mathbf{F}^{k+1} - \mathbf{F}^k\right) \\ \mathbf{Z}^{k+1} - \mathbf{Z}^{k+1} - \frac{\tau^{k+1}-\tau^k}{6}\left(\mathbf{F}^{k+1} + 4\overline{\mathbf{F}}^{k+1} + \mathbf{F}^k\right) \end{bmatrix} = \mathbf{0}$$

for a total of $8(M-1)$ equations.

REFERENCES

[1] M. Ruiz, E. Ahedo, C. Bombardelli, I. Urdampilleta, M. Merino, and F. Cichocki, "The FP7 LEOSWEEP project: improving Low Earth Orbit Security with Enhanced Electric Propulsion," *Space Propulsion Conference*, 2014.

[2] C. Bombardelli and J. Peláez, "Ion beam shepherd for contactless space debris removal," *Journal of Guidance, Control, and Dynamics*, Vol. 34, No. 3, 2011, pp. 916–920.

[3] T. Rupp, T. Boge, R. Kiehling, and F. Sellmaier, "Flight dynamics challenges of the german on-orbit servicing mission DEOS," *21st International Symposium on Space Flight Dynamics*, 2009.

[4] D. F. Lawden, *Optimal trajectories for space navigation*. Butterworths, 1963.

[5] J.-P. Marec, *Optimal space trajectories*, Vol. 1. Elsevier, 2012.

[6] C. D. Hall and V. Collazo-Perez, "Minimum-time orbital phasing maneuvers," *Journal of guidance, control, and dynamics*, Vol. 26, No. 6, 2003, pp. 934–941.

[7] P. Palmer, "Reachability and optimal phasing for reconfiguration in near-circular orbit formations," *Journal of Guidance, Control, and Dynamics*, Vol. 30, No. 5, 2007, p. 15421546.

[8] R. Bevilacqua, "Analytical guidance solutions for spacecraft planar rephasing via input shaping," *Journal of Guidance, Control, and Dynamics*, Vol. 37, No. 3, 2014, p. 10421047.

[9] W. Clohessy and R. Wiltshire, "Terminal guidance system for satellite rendezvous," *Journal of the Aerospace Sciences*, Vol. 27, No. 9, 1960, pp. 653–658. DOI: 10.2514/8.8704.

[10] J. T. Betts, *Practical Methods for Optimal Control and Estimation Using Nonlinear Programming, Second Edition*. SIAM, 2010.

[11] T. F. Coleman, B. S. Garbow, and J. J. Moré, "Software for Estimating Sparse Hessian Matrices," *ACM Transactions on Mathematical Software*, No. 11, 1985, pp. 363–377.

[12] A. E. Bryson and Y.-C. Ho, *Applied Optimal Control. Optimization, Estimation and Control.* Taylor & Francis, 1975.